

Magnetic Anisotropy in Thin Films of FePt Detected by the Ferromagnetic Resonance Method

A. I. Dmitriev^{a, b, *}, A. V. Kulikov^a, I. F. Gilmutdinov^c, N. N. Dremova^a, A. A. Mazitov^a,
M. S. Dmitrieva^{a, b}, S. I. Alekseev^d, and V. G. Myagkov^e

^aInstitute of Problems of Chemical Physics, Russian Academy of Sciences, Chernogolovka, Moscow oblast, 142432 Russia

^bRussian University of Transport, Moscow, 127994 Russia

^cKazan Federal University, Kazan, 420008 Russia

^dPlekhanov Russian University of Economics, Moscow, 117997 Russia

^eKirensky Institute of Physics, Siberian Branch, Russian Academy of Sciences, Krasnoyarsk, 660036 Russia

*e-mail: aid@icp.ac.ru

Received March 15, 2018; revised June 23, 2018; accepted June 23, 2018

Abstract—FePt thin films are made via the heat treatment of structures containing Pt (001) and Fe (001) epitaxial layers. X-ray spectral analysis and field-emission scanning electron microscopy show that the samples contain the cubic L1₂–Fe₃Pt phase and the tetragonal L1₀–FePt phase. The magnetic anisotropy of the thin films is studied by ferromagnetic resonance and magnetometric methods. The contributions from the cubic and tetragonal phases to the ferromagnetic-resonance spectrum of the sample are distinguished. The key characteristics of thin films which determine their practical applicability are determined: the Gilbert damping parameter $G \sim 0.4$, the first and second crystal anisotropy constants $K_{1\perp} = -4.08 \times 10^6$ erg/cm³, $K_{2\perp} = 1.34 \times 10^6$ erg/cm³, $K_{2\parallel} = -9.76 \times 10^4$ erg/cm³.

Keywords: FePt thin films, ferromagnetic resonance, magnetic anisotropy

DOI: 10.1134/S102745101902006X

INTRODUCTION

Traditionally, ferromagnetic resonance (FMR) is successfully applied in investigations of thin ferromagnetic films [1]. This method allows the basic characteristics of a material to be measured: damping parameter, gyromagnetic ratio, and magnetic anisotropy constants, which determine its applicability. For example, spin-transport heterostructures benefit from a low damping parameter, because it allows a decrease in the current of magnetization switching of the free layer (and hence the power consumption) and increase in the signal-to-noise ratio [2, 3]. On the contrary, the read heads of memory devices using magnetoresistive sensors should possess a high value of the damping parameter to improve the thermal stability of these devices [3, 4]. The magnetic-anisotropy constant is critical for materials from which memory devices are made. Increasing the data recording density is achieved by decreasing the size of domains, which correspond to individual bits. If the domain is too small, then the energy of thermal fluctuations may exceed the magnetic-anisotropy energy, which will result in flipping of the magnetization vector and loss of information. Materials with a high value of the mag-

netic anisotropy are needed to avoid spontaneous relaxation.

The tetragonal phase of L1₀–FePt iron–platinum alloy is one of the materials of this kind. Its magnetic anisotropy constant is larger than 10^7 erg/cm³ [5]. In principle, this is enough to make a bit size as small as 3 nm and achieve an information density of more than 1 Tb/inch² [6, 7]. Moreover, the easy magnetization axis of thin films of FePt is normal to its surface (so called perpendicular magnetic anisotropy) [7], which allows its use in the perpendicular magnetic recording technology, when bits are magnetized normally to the surface of the film medium. This technology provides a way to achieve superdense information recording.

Earlier, torque curves for FePt films were measured on a torsional magnetometer [8, 9]. The torque curves in the planes showed that there was a special type of anisotropy in FePt films (rotational magnetic anisotropy), which can be characterized by a shift $\pm L_{\text{rot}}$ of the rotational torque when the magnetic field is rotated clockwise (+) and anticlockwise (–) [8]. Rotational magnetic anisotropy is notable for the fact that the orientation of the easy magnetization axis can be “adjusted” using an external magnetic field [8, 10]. As a rule, rotational magnetic anisotropy is caused by the

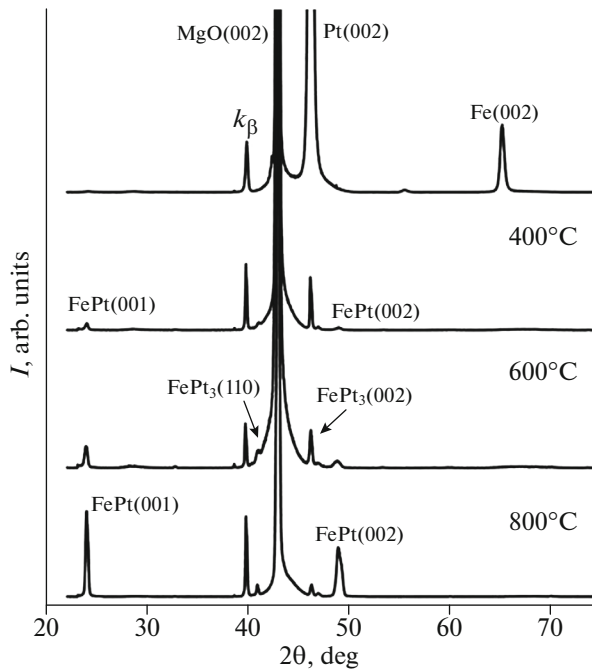


Fig. 1. X-ray spectrum of thin films of FePt.

presence of stripe-domains [11, 12]. In ferromagnetic films of FePt the rotational magnetic anisotropy may be due to the exchange interaction between the $L1_0$ -FePt and $L1_2$ -Fe₃Pt phases [8].

This paper presents the results of FMR and magnetometric studies of the magnetic anisotropy of FePt thin films, which were obtained by the heat treatment of heterostructures containing epitaxial layers of Pt(001) and Fe(001) [8]. The aim of the work is to separate the contributions from the cubic phase $L1_2$ -Fe₃Pt and tetragonal phase $L1_0$ -FePt to the FMR spectrum and to determine the basic properties of FePt thin films (damping parameter and magnetic-anisotropy constant), which define its possible practicality.

EXPERIMENTAL

Thin films of FePt were synthesized in several steps. First, a two-layer heterostructure Pt/Fe was created by consecutive thermal deposition onto a single-crystal substrate made of MgO(001). Then the obtained heterostructure Pt(001)/Fe(001)/MgO(001) was subject to step-by-step annealing in vacuum (10^{-6} Torr) at temperatures from 400 to 800°C in steps of 50°C and an exposure time of 90 min. The formed phases were identified using a DRON-4-07 diffractometer (Fig. 1). The method of preparation and attestation of the samples is described in detail in [8]. In particular, it was found in [8] that annealing at 500°C facilitates the appearance of an intermediate layer consisting of two phases on the Pt(001)/Fe(001) interface: the

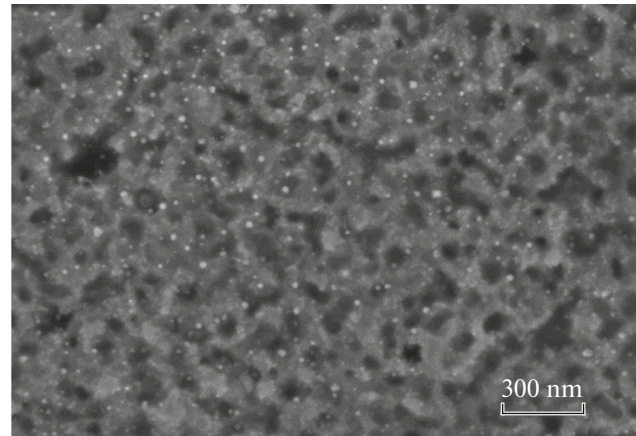


Fig. 2. Image of the surface of the FePt thin film obtained using a scanning electron microscope.

ordered cubic phase $L1_2$ -Fe₃Pt and the non-stoichiometric tetragonal phase $L1_0$ -FePt. Thus, the Pt(001)/(Fe₃Pt + FePt)/Fe(001) heterostructure was investigated in the present work.

The morphology of the FePt thin films was studied using a Zeiss SUPRA 25 field-emission scanning electron microscope. The sample has a nonuniform, grained microstructure (Fig. 2). Two types of grains are observed on its surface: bright spots with a typical size of 20 nm and dark spots with a typical size of 100 nm. We can suppose that these grains arise due to the formation of two phases: the ordered cubic phase $L1_2$ -Fe₃Pt and the nonstoichiometric tetragonal phase $L1_0$ -FePt.

The dependences of the magnetic moment of the FePt thin film on the magnetic-field intensity were measured using the method of vibrational magnetometry by a multipurpose measuring system PPMS-9 (Quantum Design) with a superconducting magnet. The measurements were carried out at a temperature of $T = 300$ K in magnetic fields up to 90 kOe in two orientations: with the film plane parallel or perpendicular to the magnetic-field lines.

The dependences of the FMR spectrum in the FePt thin film on the angle θ between the film normal and the constant magnetic field at $T = 300$ K were acquired using a Bruker ELEXSYS-II E500 electron-paramagnetic-resonance spectrometer (X-band, 9.4 GHz) equipped with an ER4103TM cylindrical resonator. The FMR spectra were recorded with a super-high frequency field power of 0.63 mW and a modulation amplitude of 5 Oe, which provided the absence of resonance saturation effects. The frequency of the magnetic-field modulation was 100 kHz. The orientation dependence of the FMR spectra was measured with the aid of an ER 218PG1 programmable goniometer. Rotation of the FePt films was achieved by rotating the substrate about the [110] axis. The FMR spectra were obtained as dependences

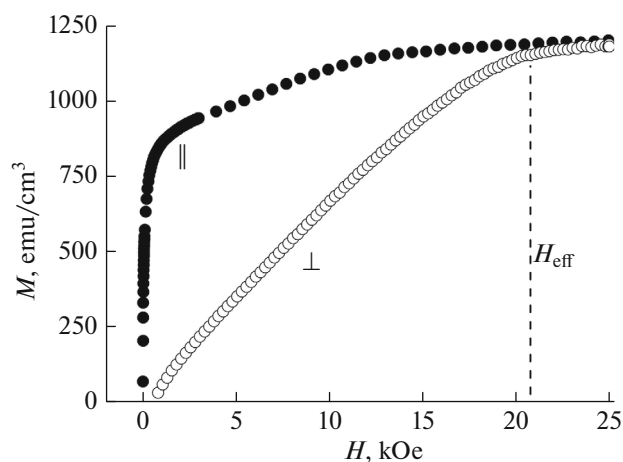


Fig. 3. Field dependences of the magnetization of the FePt thin film. Filled symbols correspond to the film plane oriented parallel to the magnetic field; empty symbols correspond to the perpendicular orientation. The vertical dashed line points to the effective magnetic field H_{eff} .

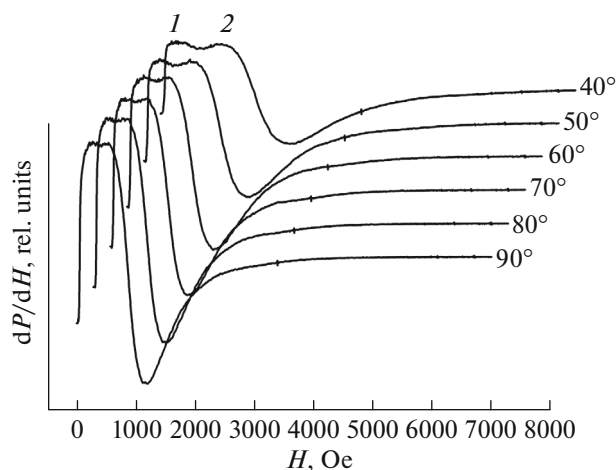


Fig. 4. FMR spectra of the FePt thin film at different orientations of its plane relative to the magnetic field. Resonance peaks are marked with numbers.

of the first derivative of the absorbed power with respect to the magnetic field (dP/dH) on the value of the magnetic field, which varied from 0 to 10 kOe.

RESULTS AND DISCUSSION

Figure 3 shows the field dependences $M(H)$ of the FePt-thin-film magnetization measured at two orientations of the magnetic field: parallel and perpendicular to the film plane. The shape of the $M(H)$ curve is typical of a ferromagnetic with prominent magnetic anisotropy. The field value at which both curves coincide is the effective field in the sample, $H_{\text{eff}} = 22$ kOe. In turn, it consists of two components: the demagnetizing field ($4\pi M_s$) and the anisotropy field H_a [13].

The magnetic-anisotropy field was estimated as $H_a = 6.7$ kOe based on the saturation magnetization $M_s = 1220$ emu/cm³ (Fig. 3). Using the relation $H_a = 2K/M_s$, we can estimate the magnetic-anisotropy constant as $K = 4.07 \times 10^6$ erg/cm³. The values of the saturation magnetization and magnetic-anisotropy constant differ remarkably from those observed in Fe films [14] and are close to the corresponding values for the nonstoichiometric tetragonal phase $L1_0$ -FePt. A noteworthy fact is the value of K obtained here which is smaller than the known value $>10^7$ erg/cm³. This can be due to the presence of a soft-magnetic, weakly anisotropic cubic phase $L1_2$ -Fe₃Pt and/or partial amorphization of the sample. The magnetization curves $M(H)$ recorded in the film plane (Fig. 3) show a “step” ending at $H \approx 10$ kOe. Peculiarities of this kind on the $M(H)$ dependences were observed earlier in other systems consisting of a mix of a hard- and soft-magnetic phases [15]. In order to separate the contributions of these phases to the net magnetic moment, a procedure described in [15] can be used; however, using the FMR technique is more effective.

The FMR spectra recorded in the FePt thin film at different orientations of the constant magnetic field with respect to its plane is shown in Fig. 4. A spectrum contains two lines at resonance frequencies near 0.6 kOe (line 1) and 2 kOe (line 2). The mentioned values of H_{res} correspond to the angle $\theta = 30^\circ$ between the film plane and the constant magnetic field. The width ΔH and resonance field H_{res} of both lines depend on the orientation of the film plane relative to the constant magnetic field, and their shape is typical of FMR. At $\theta \rightarrow 0^\circ$ the value H_{res} tends to $H_{\text{eff}} = 22$ kOe, and thus spectra could not be recorded at small angles because the resonance field was outside the magnetic-field sweep range (from 0 to 10 kOe). The integrated intensity of line 2 is almost one order of magnitude larger than the intensity of line 1. High saturation magnetization points to the fact that the main phase of the sample is the tetragonal $L1_0$ -FePt phase, and hence it is reasonable to assign line 1 to the cubic phase $L1_2$ -Fe₃Pt, and line 2 to the tetragonal phase $L1_0$ -FePt. The integral contribution of line 1 (from the cubic phase $L1_2$ -Fe₃Pt) is little, and thus we will discuss further only line 2 (from the tetragonal phase $L1_0$ -FePt). We note that one could expect to observe a third line in the FMR spectrum corresponding to pure Fe, which was not involved in the solid-state chemical reaction. The absence of it in the spectra means that the volume fraction of pure Fe is negligible; this is proved also by X-ray analysis (Fig. 1).

To determine the contribution of line 2 to the FMR spectrum, it was approximated (Fig. 5). The motion of the magnetization vector \mathbf{M} in solids, allowing for dissipation, is described by the Landau–Lifshitz–Gilbert equation [16]:

$$\frac{\partial \vec{M}}{\partial t} = -\gamma [\vec{M} \times \vec{H}_{\text{eff}}] + \frac{G}{M} \left[\vec{M} \times \frac{\partial \vec{M}}{\partial t} \right], \quad (1)$$

where γ is the gyromagnetic ratio, H_{eff} is the effective magnetic field, G is the relaxation Gilbert parameter (damping parameter) which is related to the FMR line width and the resonance field: $G = \Delta H / H_{\text{res}}$ [12]. Equation (1) corresponds to a resonance-line shape described by the following equation [16]:

$$\frac{dP}{dH} \propto \frac{d}{dH} \times \left(\frac{\Delta H (H^2 + H_{\text{res}}^2 + \Delta H^2) H}{[(H - H_{\text{res}})^2 + \Delta H^2][(H + H_{\text{res}})^2 + \Delta H^2]} \right), \quad (2)$$

where ΔH is the FMR line width and H_{res} is the resonance field. The FMR spectrum in the FePt thin film was approximated by the sum of two lines given by Eq. (2) (Fig. 5). The values of H_{res} and ΔH for each orientation of the thin film were determined from the approximation. With the values found this way ($H_{\text{res}} \sim 822$ Oe and $\Delta H \sim 387$ Oe, obtained for $\theta = 90^\circ$), we can estimate the Gilbert relaxation parameter to be $G_{\perp} \sim 0.4$.

The dependence of the resonance field H_{res} of FMR line 2 in the FePt thin film on angle θ is plotted in Fig. 6. The orientation dependence $H_{\text{res}}(\theta)$ is caused by the magnetic anisotropy. Usually a rotating field H_{rot} (field of rotational anisotropy) is introduced in papers dedicated to FMR studies of rotational magnetic anisotropy, which expresses the energy of the rotational magnetic anisotropy in units of magnetic-field intensity. The orientation dependence $H_{\text{res}}(\theta)$ is fitted by the correlation $H_{\text{dyn}} = H_{\text{stat}} \cos 2\theta + H_{\text{rot}}$ [17]. Here H_{dyn} is the dynamic field of the magnetic anisotropy, measured by the FMR method (it is equivalent to the resonance field H_{res}); H_{stat} is the static field defined by the contribution of the crystalline anisotropy. The H_{rot} term is angle independent since rotational magnetic anisotropy does not depend on the crystalline field or spin-orbit interaction. An attempt to approximate the dependence $H_{\text{res}}(\theta)$ by the expression for H_{dyn} is shown in Fig. 6 by a light curve. The values of the static and dynamic magnetic-anisotropy fields determined from the approximation are $H_{\text{stat}} = 1.7$ and $H_{\text{dyn}} = 1.9$ kOe, respectively; thus, the contribution of rotational magnetic anisotropy can exceed 50%. We note also that the expression for H_{dyn} provides low-quality fitting of the dependence $H_{\text{res}}(\theta)$ (see Fig. 6); at least, this approximation is notably worse than in other investigations. Therefore, in what follows we decided to use a traditional procedure to analyze the magnetic anisotropy in magnetic films.

The dependence of the resonance field for a ferromagnetic film having tetragonal symmetry on the polar θ and azimuthal φ angles, taking into account the first ($K_{1\perp}$, $K_{1\parallel}$) and second ($K_{2\perp}$, $K_{2\parallel}$) constants of crystalline anisotropy, can be derived from the free energy which is given as follows [18]:

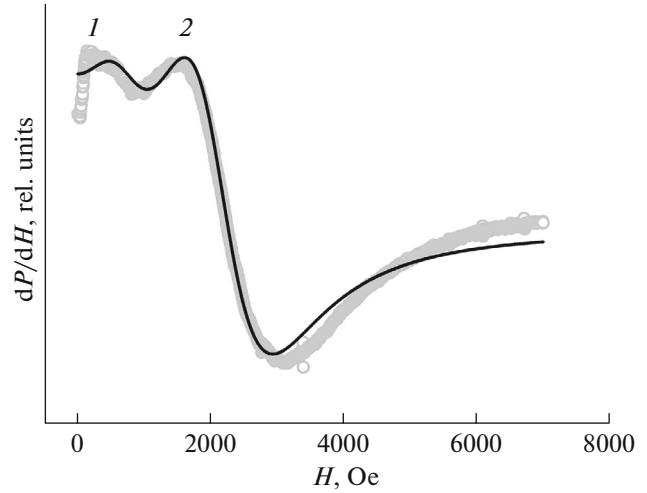


Fig. 5. Experimental (dots) and calculated (curve) FMR spectra in the FePt thin film at an angle of 30° between the normal to its surface and a constant magnetic field. Resonance peaks are marked with numbers.

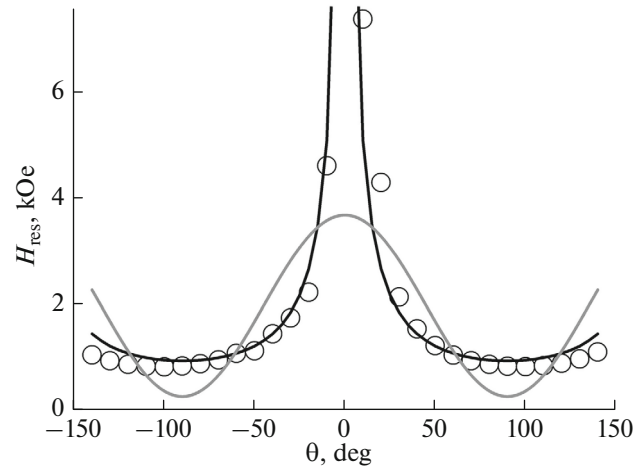


Fig. 6. Dependence of the resonance field of FMR line 2 in the FePt thin film on the angle between the normal to its surface and a constant magnetic field. Approximation results are plotted as solid lines.

$$E = -\vec{H}\vec{M} - (K_{1\perp} - 2\pi M_s^2) \cos^2 \theta - \frac{1}{2} K_{2\perp} \cos^4 \theta - \frac{1}{2} K_{2\parallel} \frac{1}{4} (3 + \cos 4\varphi) \sin^4 \theta + K_{1\parallel} \sin^2 \theta \cos^2(\varphi - \varphi_{2\parallel}). \quad (3)$$

The resonance angular frequency ω is written as follows [14]:

$$\left(\frac{\omega}{\gamma} \right)^2 = \frac{1}{M_s^2} \times \left[E_{\theta\theta} \left(\frac{E_{\varphi\varphi}}{\sin^2 \theta} + \frac{\cos \theta}{\sin \theta} E_\theta \right) - \left(\frac{E_{\theta\varphi}}{\sin \theta} - \frac{\cos \theta}{\sin \theta} \frac{E_\varphi}{\sin \theta} \right)^2 \right], \quad (4)$$

where E_θ , E_φ , $E_{\theta\theta}$, $E_{\varphi\varphi}$, $E_{\theta\varphi}$ are the first and second partial derivatives of the free energy (3) with respect to the corresponding angles. Differentiation of Eq. (3) and substitution of the derivatives in (4) yields an expression showing the angular dependence $H_{\text{res}}(\theta)$ as an implicit function. It is rather cumbersome and hence is not written here. Approximation of the experimental dependence of the resonance field H_{res} of line 2 on the angle θ gives the following values of the constant of crystalline anisotropy: $K_{1\perp} = -4.08 \times 10^6$, $K_{2\perp} = 1.34 \times 10^6$, and $K_{2\parallel} = -9.76 \times 10^4$ erg/cm³ (dark line in Fig. 6).

CONCLUSIONS

The magnetic anisotropy in thin films of FePt was investigated by FMR and magnetometric methods. The FMR spectrum was found to contain two anisotropic resonance lines, one of which corresponds to the cubic phase $\text{L1}_2\text{-Fe}_3\text{Pt}$, and the other belongs to the tetragonal phase $\text{L1}_0\text{-FePt}$. Approximation of the spectra based on the Landau–Lifshitz–Gilbert equation allowed determination of the Gilbert damping parameter $G_\perp \sim 0.4$. The dependence of the FMR line position H_{res} of the tetragonal phase on the polar angle θ was studied. Approximation of $H_{\text{res}}(\theta)$ by the corresponding equation yielded the first and second constants of magnetic anisotropy: $K_{1\perp} = -4.08 \times 10^6$, $K_{2\perp} = 1.34 \times 10^6$, and $K_{2\parallel} = -9.76 \times 10^4$ erg/cm³. The contributions of crystalline anisotropy and shape anisotropy of the FePt thin films were distinguished.

ACKNOWLEDGMENTS

The study was performed under state contract no. 007-00160-18-00. The dependences of the magnetic moment of the samples on the magnetic-field intensity were measured using instruments of the Federal center for shared facilities for the physical-chemical research of compounds and materials at Kazan Federal University.

REFERENCES

1. M. Farle, Rep. Prog. Phys. **61**, 755 (1998).
2. N. Smith and P. Arnett, Appl. Phys. Lett. **78**, 1448 (2001).

3. T. A. Ostler, M. O. A. Ellis, D. Hinzke, and U. Nowak, Phys. Rev. B **90**, 094402 (2014).
4. S. Maat, N. Smith, M. J. Carey, and J. R. Childress, Appl. Phys. Lett. **93**, 103506 (2008).
5. O. A. Ovanov, L. V. Solina, and V. A. Demshina, Phys. Met. Metallogr. **35**, 81 (1973).
6. H. Dang, L. Liu, L. Hao, T. Jin, M. Liu, J. Cao, J. Bai, Y. Wang, and F. Wei, J. Appl. Phys. **115**, 17B711 (2014).
7. A.-C. Sun, P. C. Kuo, J.-H. Hsu, H. L. Huang, and J.-M. Sun, J. Appl. Phys. **98**, 076109 (2005).
8. V. S. Zhigalov, V. G. Myagkov, L. E. Bykova, G. N. Bondarenko, A. A. Matsynin, and M. N. Volochaev, Phys. Solid State **59**, 392–398 (2017).
9. V. S. Zhigalov, V. G. Myagkov, L. E. Bykova, G. N. Bondarenko, D. A. Velikanov, and M. N. Volochaev, Phys. Solid State **60**, 178–182 (2018).
10. V. G. Myagkov, V. S. Zhigalov, L. E. Bykova, G. N. Bondarenko, A. N. Rybakova, A. A. Matsynin, I. A. Tamasov, M. N. Volochaev, and D. A. Velikanov, JETP Lett. **102**, 355 (2015).
11. S. Tacchi, S. Fin, G. Carlotti, G. Gubbiotti, M. Madami, M. Barturen, M. Marangolo, M. Eddrief, D. Bisero, A. Rettori, and M. G. Pini, Phys. Rev. **89**, 024411 (2014).
12. G. Wang, C. Dong, W. Wang, Z. Wang, G. Chai, C. Jiang, and D. Xue, J. Appl. Phys. **112**, 093907 (2012).
13. E. Burgos, E. S. Leva, J. Gomez, F. M. Tabares, M. V. Mansilla, and A. Butera, Phys. Rev. B **83**, 174417 (2011).
14. Y. Nagai, A. Tago, K. Yanagisawa, and T. Toshima, J. Appl. Phys. **61**, 3841 (1987).
15. E. N. Kablov, O. G. Ospennikova, D. E. Kablov, V. P. Piskorskii, R. A. Valeev, D. V. Korolev, I. I. Rezchikova, E. I. Kunitsyna, A. D. Talantsev, A. I. Dmitriev, and R. B. Morgunov, J. Exp. Theor. Phys. (JETP) **121**, 429 (2015).
16. T. L. Gilbert, IEEE Trans. Magn. **40**, 3443 (2004).
17. G. Chai, N. N. Phuoc, and C. K. Ong, Sci. Rep. **2**, 832 (2012).
18. B. Schulz and K. Baberschke, Phys. Rev. B **50**, 13467 (1994).

Translated by S. Efimov